Spectroscopic techniques in the study of human tissues and their components. Part I: IR spectroscopy

Sylwia Olsztyńska-Janus[1,2]*, Katarzyna Szymborska-Małek[3],
Marlena Gąsior-Głogowska[1,2], Tomasz Walski[1,2],
Małgorzata Komorowska[1,2], Wojciech Witkiewicz[2], Celina Pezowicz[2,4],
Magdalena Kobielarz[2,4], Sylwia Szotek[4]

[1] Institute of Biomedical Engineering and Instrumentation, Wrocław University of Technology, Poland.
[2] Regional Specialist Hospital in Wrocław, Research and Development Centre, Wrocław, Poland.
[3] Institute of Physical and Theoretical Chemistry, Wrocław University of Technology, Poland.
[4] Division of Biomedical Engineering and Experimental Mechanics, Wrocław University of Technology, Poland.

Among the currently used methods of monitoring human tissues and their components many types of research are distinguished. These include spectroscopic techniques. The advantage of these techniques is the small amount of sample required, the rapid process of recording the spectra, and most importantly in the case of biological samples – preparation of tissues is not required. In this work, vibrational spectroscopy: ATR-FTIR and Raman spectroscopy will be used. Studies are carried out on tissues: tendons, blood vessels, skin, red blood cells and biological components: amino acids, proteins, DNA, plasma, and deposits.

Key words: *vibrational spectroscopy, ATR-FTIR, Raman, tissues*

1. Introduction

Development of research methods provides opportunities for monitoring biomedical changes and metabolic processes with the use of various spectroscopic techniques. At present, there are a lot of spectroscopic methods based on various effects of interactions between radiation and matter, among which vibrational spectroscopy deserves special attention. The method is widely used for gathering structural information on biological systems during *in situ* and *in vivo* investigations. It is non-invasive and causes no damage to experimental materials. The method helps identify tissues and their components as well as investigate their mutual interactions. Vibrational spectroscopy can be applied for quantitative and qualitative analyses. It can be used for studying materials in different physical states and requires no (or slight) sample preparation or chemical modifications.

The infrared and Raman spectroscopies are used as complementary techniques. Interpretation of IR and Raman bands is based on a comparative analysis of spectra corresponding to investigated materials and the standard substance spectra. In general, a spectral analysis is based on identification of band positions in obtained spectra, assignment of specific bands to corresponding bonds and functional groups as well as observation of spectral parameter changes.

2. ATR-FTIR spectroscopy

Water in biological fluids and tissues has a very high molar absorptivity in the infrared region, such that many of the water absorption bands are so intense that they cannot be reliably measured using standard transmission techniques. In such cases ATR technique may be preferable [1]. ATR-FTIR (Attenuated Total Reflection Fourier Transform Infrared Spectroscopy) spectroscopy is a technique of infrared spectroscopy using the phenomenon of the attenuated total internal reflection of electromagnetic radiation on the crystal/sample interface. ATR method offers the important advantage of being non-destructive, requiring micrograms of material and no (or small) sample preparation.

ATR method has become an accepted tool in biomedical sciences, providing information concerning the structure and interactions of amino acids, proteins, lipids, carbohydrates and nucleic acids in isolation and as components of tissues. Studies of these samples in the fingerprint regions of ATR spectra have generated a great deal of valuable biochemical information about their structure and interactions [2]. Currently available ATR-FTIR spectrometers can provide reproducible IR spectra of tissue components in solutions, on surfaces and under aqueous conditions.

2.1. DNA

The study of aqueous DNA solutions by infrared spectroscopy requires extremely limited water content in the sample due to strong absorption of radiation by the solvent (about 1640 cm^{-1}). An analysis of such spectra may be difficult due to the overlapping of water and nucleic acid bands. As a result of the limitations regarding water content in the sample, high concentrations of nucleic acid solutions are required. This can lead to deformation of a spectrum due to intermolecular interactions. The use of thin films or powders of DNA can solve these problems. Despite these limitations, the method can provide valuable information about the DNA structure [3].

The IR spectra of DNA show many characteristic bands, which are sensitive to denaturation, dehydration and conformational transition. The infrared spectrum can be divided into four characteristic spectral ranges: base, base-sugar, sugar-phosphate and sugar vibrations (figure 1). Within the 1800–1500 cm^{-1} region, there are absorption bands associated with C=O, C=N, C=C stretching vibrations and N–H bending vibrations of bases. These bands are sensitive to changes in the base stacking and base pairing interactions. Bands occurring in the interval 1500–1250 cm^{-1} are assigned to vibrations of the bases and base-sugar connections. The range of 1250–1000 cm^{-1} refers to vibrations of a phosphate-sugar chain. The bands within this range, including PO_2^- symmetric and asymmetric stretching vibrations as well as C–O stretching vibrations of the side chain, show high sensitivity to conformational changes of the backbone. Within the last region (1000–800 cm^{-1}), there are absorption bands associated with sugar vibrations, which correlate with the various nucleic acid sugar puckering modes (C2′-endo and C3′-endo) [4]–[9].
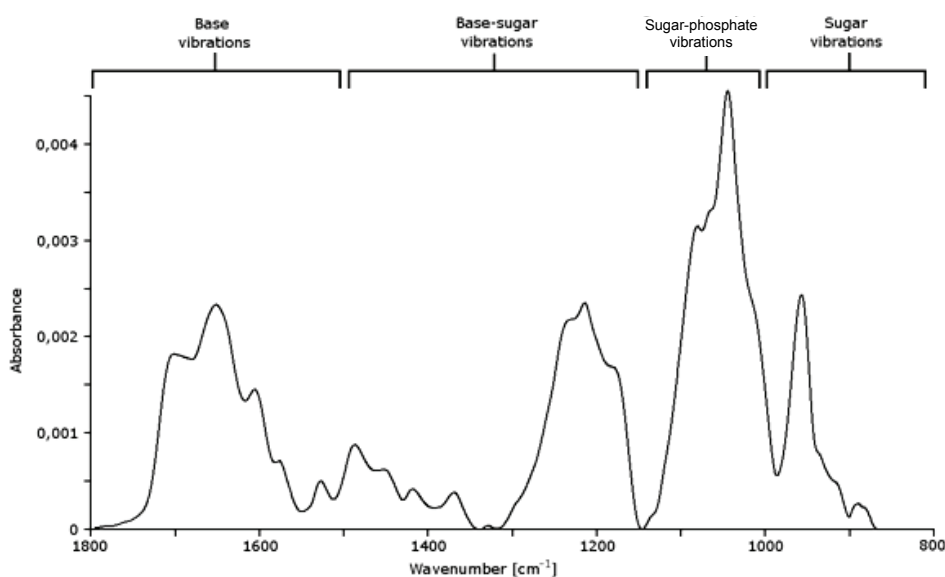

Fig. 1. The FTIR-ATR spectrum of herring sperm DNA films in the interval 850–1800 cm^{-1}.
Labels identify bands assigned to specific base, sugar and phosphate vibrations

2.1.1. DNA hydration

It is well known that water is a key factor regarding stabilization of secondary and tertiary biopolymer structures [10]. Structural modifications of water surrounding a biomolecule result in conformational changes and, as a consequence, lead to modulation of their functions and properties. In the case of nucleic acids, water and hydrated ions neutralize electrostatic repulsions between phosphate groups. DNA stability and conformational diversity mainly depend on interactions with surrounding water molecules [11]. Due to a highly ionic character of nucleic acids, the strength of interactions between these biomolecules and water molecules is far greater than for proteins. Hydration of nucleic acids can be described with three hydration layers [12], [13]. The first layer is impermeable to ions and remains in a close contact with a polyelectrolyte molecule. For the DNA double helix, at the relative humidity (RH) of about 92%, approximately 20 water molecules per nucleotide form the primary hydration layer. However, as demonstrated in many studies, only 10–12 water molecules per nucleotide directly interact with the phosphates, oxygen atoms in sugars as well as polar groups of bases are incapable of crystallization to ice upon cooling to temperatures well below 0 °C [9], [12]–[16]. Bound water is important for macromolecule stability and its removal results in the structure disruption [9], [17]. With high water activity (high relative humidity), all oxygen atoms of phosphate groups, oxygen atoms of sugars and functional groups of bases are highly hydrated [16], [18]. In this case, DNA appears in the B-type conformation. When the water activity decreases, its molecules are removed from the helix and the DNA conformation changes, resulting in fewer water molecules required for structure hydration. The conformation of sugar is changed from C2′-endo to C3′-endo and within the same strand, the distance between adjacent phosphate groups is decreased. Hydration becomes more economical and DNA is transformed into the A-type [11], [14], [15], [19]. Further dehydration results in removal of remaining water molecules that interact with bases and sugars, whereas phosphate groups are still hydrated. Such DNA dehydration leads to disruption of stacking interactions between the bases and consequently degradation of the macromolecule.

Infrared spectroscopy has proven to be a perfect tool for investigating the effects of hydration levels on the DNA structure [9]. The consequence of DNA dehydration from 95% to 88% RH is its transition from the B-type into the A-DNA. The process is accompanied by infrared spectral changes. The B-DNA is characterized by the presence of 835, 1088, 1223 and 1715 cm^{-1} marker bands. In the A-type of 88% relative humidity, the bands are shifted to 861, 1089, 1234 and 1709 cm^{-1}, respectively. Moreover, the A-DNA infrared spectrum contains a new band at 1185 cm^{-1} assigned to the vibrations of deoxyribose in the C3′-endo conformation [5], [20]. Further dehydration of a DNA molecule leads to the loss of its ordered structure, which is manifested by decreased intensities of bands in the 1709–1715 cm^{-1} region. In DNA samples with the water content of 7.2, 3.3 and 1.2 wpn, the band in this region disappears, which indicates the loss of interactions between bases and partial DNA denaturation [9]. DNA dehydration results in changes within other infrared bands. Due to dehydration, strong shifts of bands corresponding to the PO_2^- asymmetric stretching vibrations from 1220 cm^{-1} (95% RH) to 1240 cm^{-1} (0% RH), PO_2^- symmetric stretching vibrations from 1089 cm^{-1} (95% RH) to 1086 cm^{-1} (0% RH), C–O stretching vibrations of the side chain from 1052 cm^{-1} (95% RH) to 1066 cm^{-1} (0% RH) and C–C stretching vibrations of the backbone from 970 cm^{-1} (95% RH) to 962 cm^{-1} (0% RH) are observed. The changes within these bands prove that dehydration of the macromolecule results in destruction of ordered DNA structure [21].

2.1.2. DNA denaturation

Infrared spectroscopy is an effective tool for investigating nucleic acid denaturation, i.e., separation of a double-stranded DNA into two individual strands. The process is accompanied by intensity changes and shifts of many bands in the infrared spectrum. The most significant changes occur within vibrations of the C=O and C=N groups of bases. Thermal denaturation of DNA results in disruption of hydrogen bonds between base pairs. In the infrared spectrum, a shift of the band from 1710 cm^{-1} (double helix of DNA) to 1690 cm^{-1} (denatured DNA) is observed. However, this band should be analyzed with great caution in the case of spectra recorded for aqueous DNA solutions. The band may be overlapped by a band corresponding to vibrations of the hydroxyl groups (–OH) of DNA-bonded water [3]. The denaturation process is also accompanied by changes within other infrared bands [4], [8], [9]. The bands sensitive to temperature changes are listed in table 1.

Table 1. Major positions (in cm^{-1}) and tentative assignment
of IR bands of aqueous B-DNA.
Spectral changes observed during denaturation of DNA

ν [cm^{-1}]		Changes in band parameters	Assignments*
1715	(–)	1690 cm^{-1}	ν(C=O), ν(C=C) ν(C=N), β(N–H)
1664	(–)	1649 cm^{-1} disappearance of the band splitting	
1610	(–)	1607 cm^{-1}	
1492		1487 cm^{-1}	β(NH/CH) of A, G
1425	(–)	1410 cm^{-1}	dC2′-endo
1375	(+)	1362 cm^{-1}	d purine/anti
1292		disappear	ν(C$_4$NH$_2$) of C
1225	(–)	1240 cm^{-1}	ν_{as}(PO$_2^-$)
1088	(–)	1096 cm^{-1}	ν_s(PO$_2^-$)
1050	(+)	1069 cm^{-1}	ν(C–O)b
970	(–)	957 cm^{-1}	ν(C–C)b
894	(–)	883 cm^{-1}	δd
835	(–)	819 cm^{-1}	ν(O–P–O)b

*Abbreviations: ν, stretching; β, in-plane bending; δ, in-plane bending (ring); γ, out-of-plane bending; s, symmetrical; as, asymmetrical; A, adenine; T, thymine; G, guanine; C, cytosine; d, deoxyribose; b, backbone. Plus (or minus) sign indicates that the band has gained (or lost) appreciable intensity as a result of DNA melting.

2.1.3. Interactions with metals

Metal ions give rise to various structural changes within a DNA molecule, including B-DNA → A-DNA, B-DNA → A-DNA → Z-DNA, B-DNA → C-DNA → Z-DNA, B-DNA → Z-DNA and B-DNA → Z-DNA → ΨDNA transitions. Moreover, aggregation and condensation of a macromolecule, helix stabilization or denaturation and structural changes like helix-coil transition are observed [22]. As shown in many studies, metals with a high affinity to bases destroy hydrogen bonds between base pairs, which leads to destabilization of B-DNA molecule [22]. On the other hand, cations that preferentially interact with phosphate groups stabilize the B-DNA structure due to neutralization of the phosphate negative charge. Metal ions with increasing affinity to bases can be ordered as follows: Hg^{2+} > Cu^{2+} > Pb^{2+} > Cd^{2+} > Zn^{2+} > Mn^{2+} > Ni^{2+}, Co^{2+} > Fe^{2+} > Ca^{2+} > Mg^{2+}, Ba^{2+}. All of them, excluding Hg^{2+}, more easily bind to GC than AT pairs [22].

IR spectroscopic studies [23] on DNA-Ca^{2+}, DNA-Mn^{2+} and DNA-Cu^{2+} complexes have revealed that all analyzed ions, particularly Cu^{2+}, significantly change the macromolecule structure. In the IR spectra of DNA-metal ion complexes, shifts of absorption bands of phosphate groups and bases as well as the increase in their intensity are observed, which proves that metal ions interact both with the nucleic bases and phosphates. Cu^{2+} ions drastically change the B-DNA molecular structure, which results in a partial disruption of the macromolecule even with the ratio of [Cu^{2+}]/[P] > 0.36, where [P] is a molar concentration of phosphates in DNA. Ca^{2+} and Mn^{2+} ions do not change the structure of B-DNA molecule. In the IR spectrum, changes of absorption band shapes and shifts of the B-DNA marker bands are observed; for Cu^{2+} ions, a shift from 1053 to 1060–1070 cm^{-1} is seen. Moreover, within the phosphate absorption region, shifts of the 1090–1095 cm^{-1} and 1223–1230 cm^{-1} bands corresponding to the DNA-Cu^{2+} complexes can be seen. In the case of DNA molecules that interact with Ca^{2+} and Mn^{2+} ions, shifts of the above bands are significantly lower. Based on the investigations presented, ions that interact with phosphate groups can be ordered as follows: Cu^{2+} > Mn^{2+} > Ca^{2+}. Simultaneously distinct changes in IR spectra of the DNA-metal ion complexes can be observed in the absorption region of nucleic bases. In the spectra of DNA-Cu^{2+} complexes, new absorption bands at 1547 and 1590 cm^{-1}, respectively, appear even with the ratio of [Cu^{2+}]/[P] > 0.2. Additionally, for this copper ion concentration, distinct band shifts are observed: 1675 and 1650 cm^{-1} to 1662 and 1643 cm^{-1}, respectively. Their presence results from interactions of Cu^{2+} ions with N3 of cytosine and N7 of guanine. This indicates that

within the range of $0.2 < [Cu^{2+}]/[P] < 0.36$, copper ions are bound to N7 and O6 of guanine and to O_2 of cytosine.

The IR spectral analysis carried out by AHMAD et al. [24] for DNA-Mg^{2+} and DNA-Ca^{2+} complexes revealed that the band corresponding to the PO_2^- asymmetric stretching vibrations at 1222 cm^{-1} was shifted and split into three components: 1216, 1231 and 1250 cm^{-1} for Ca-DNA. In the IR spectra of Mg-DNA, however, no band shift or split was observed. Moreover, the band at 1222 cm^{-1} demonstrates a 30% increased intensity for calcium complexes and a 15% increase for magnesium complexes compared to free DNA. Additional evidence for the binding of calcium ions by phosphate groups is a change of relative intensities of bands associated with the PO_2^- symmetric v_s and asymmetric v_{as} stretching vibrations. After Ca-DNA-complex formation, the v_s/v_{as} ratio of 1.7 for free DNA decreases to 1.5, whereas after binding Mg^{2+} to DNA, no change is seen. The observed spectral changes are most probably caused by direct binding of Ca^{2+} ions and indirect binding of Mg^{2+} ions to the phosphate groups. The split observed for the 1222 cm^{-1} (1216, 1231 and 1250 cm^{-1}) band in the Ca-DNA complexes spectra may indicate multidentate Ca-phosphates bindings, probably by O1P and O2P atoms. After Mg^{2+}- and Ca^{2+}-complex formation [24], a strong guanine vibration band at 1717 cm^{-1} for free DNA [25], [26] is shifted to lower frequencies (1710 cm^{-1}). The shift is accompanied by 30% increased band intensity for Mg-DNA and a 20% increase for Ca-DNA. The observed spectral changes are associated with direct interactions of Mg ions with N7 of guanine (Mg–N7) and indirect interactions of Ca–H_2O–N7-guanine in Ca-DNA complexes. A shift of the band corresponding to guanine vibrations (1717 cm^{-1}) and the presence of a phosphate component bands at 1216 cm^{-1} (v_{as} PO_2^-) suggest that the Ca^{2+} cation forms chelate bonds with N7 of guanine and with the phosphate group of the DNA side chain. Such chelation was not observed for the Mg-DNA adducts. In these complexes, O6–H_2O–cation–N7 interactions possibly occur due to proximity of the O6 atom and the metal-binding N7 atom, which results in stabilization of the Mg-DNA complexes.

FTIR spectroscopy was also used in the studies of Cu^{2+} and Pb^{2+} effects on DNA denaturation [27]. The studies were conducted for DNA solutions of pH = 6.5 with both metal additives. The molar ratios (r) of the ions to DNA (P) (P = phosphate) were as follows: 1/80, 1/40, 1/20, 1/10, 1/4, 1/2. The experiments showed that with a low ratio of 1/80 and 1/40, both

metal ions mainly bound to the DNA phosphate groups, increasing the strength of stacking interactions between the bases and enhancing the duplex stability. With $r > 1/40$, Cu^{2+} ions are bound to the DNA molecules with GC pairs, whereas Pb^{2+} cations, at $r > 1/20$, bind to AT pairs. DNA denaturation in the presence of Cu^{2+} ions begins when $r = 1/10$ and it lasts until $r = 1/2$, whereas for a high level of the Pb^{2+} ions ($r = 1/2$), only a partial destabilization of the DNA double helix was observed. In the IR spectra of DNA solutions with Cu^{2+} and Pb^{2+} additives, DNA condensation due to the presence of both metal ions was observed. It was also noted that neither of the ions caused conformational changes of the DNA molecules. During the experiments, the B-DNA structure was maintained.

However, there are some literature reports concerning the effects of Fe(II) and Fe(III) ions on DNA denaturation detected during investigations with the use of infrared spectroscopy [28]. The experiments were conducted for DNA solutions with iron ion additives. The range of molar ratios (r) of metal ion/DNA (P) was 1/160:1/2. They showed that at low cation ratio ($r = 1/80$ and $r = 1/40$), the Fe(II) iron ions bound to N-7 of guanine and to phosphate groups of the macromolecule. Specific binding constants of cations for these groups are: $K_G = 5.40 \times 10^4$ M^{-1} and $K_P = 2.40 \times 10^4$ M^{-1}. For higher cation levels, Fe(II) ions bind to adenine N-7 and thymine O-2. The Fe(III) ions show a higher binding affinity to bases and phosphate groups of DNA than the Fe(II) ions. At low cation ratio ($r = 1/80$), Fe(III) ions primarily bind to phosphate groups, whereas at high cation levels, they bind to the phosphate groups and guanine N-7 with specific binding constants of $K_G = 1.36 \times 10^5$ M^{-1} and $K_P = 5.50 \times 10^4$ M^{-1}. When the molar ratio reaches $r = 1/10$, Fe(II) ions cause structural destabilization of DNA, while Fe(III) ions induce DNA condensation. The FTIR spectral analysis showed no conformational changes of DNA due to its interactions with the Fe(II) and Fe(III) ions.

2.1.4. The effects of pH

Many studies conducted with infrared spectroscopy related to the effects of pH on DNA have shown that protonation of DNA bases leads to helix destabilization and denaturation, resulting in structural changes within the macromolecule [27]. Protonation of cytosine (N-3) and adenine (N-1) occurs at pH of 5.3, whereas for guanine and thymine, it takes place at the pH of 9–10. The studies have shown that for low proton levels (pH 7–5), the DNA spectrum modified by H^+ ion does not signfcantly differ from the DNA spectrum recorded for pH 7. The only differences are

observed within the C=O vibrations of guanine and thymine. A band shift to lower frequencies (1712 cm^{-1}) is observed. Moreover, slightly decreased band intensities corresponding to the C6=O6 of guanine and C_2=O_2 of thymine (1717 cm^{-1}) stretching vibrations, the C_4=O_4 stretching vibrations of thymine (1662 cm^{-1}), (1609 cm^{-1}) and the vibrations within adenine and guanine rings (1492 cm^{-1}) as well as a slightly increased intensity of the band corresponding to the PO_2^- antisymmetric stretching vibrations at 1222 cm^{-1} are observed. Additionally, the decrease in band intensities associated with in-plane vibrations occurs due to increased stacking interactions between bases and enhanced helix stability in the presence of H$^+$ ions. A stronger structural stability is evidenced by an increased band intensity at 1222 cm^{-1}, which confirms the presence of interactions between the phosphate groups and H$^+$ ions. Whereas at pH < 5 protonation of bases it is manifested by increased band intensities at 1717, 1662, 1609, 1492 and 1222 cm^{-1}. At this stage, protonation of adenine and cytosine bases occurs, resulting in increased band intensities at 1609 and 1492 cm^{-1}. Protonation of cytosine and adenine is indirectly induced by interactions of H$^+$ ions (through water molecules) with the PO_2^- phosphate groups and other bases. Moreover, in the experiment increased band intensities at 1222, 1662 and 1717 cm^{-1} were observed. However, the guanine band (1717 cm^{-1}) demonstrates a greater intensity increase than the thymine band (1662 cm^{-1}). This means that at the first stage, cytosine protonation occurs followed by unpairing of GC pairs. The evidence of direct interactions of H$^+$ ions with adenine and cytosine is a shift of bands to lower frequencies: from 1609 to 1607 cm^{-1} for adenine and from 1492 to 1490 cm^{-1} for cytosine. Summing up, adenine and cytosine protonation affects interactions between the GC and AT pairs, which leads to the loss of helix stability. Further decrease of pH results in strong H$^+$ ion binding to bases and, as a consequence, DNA aggregation. The IR spectrum reveals decreased intensities of bands at 1717, 1662, 1609, 1492 and 1222 cm^{-1}. Whereas pH reduction to 2.2 causes the B-DNA→C-DNA conformational transition. In the IR spectrum, a rapid decrease in band intensities as well as splitting of the 1222 cm^{-1} band into 1220 and 1228 cm^{-1} components are observed.

2.2. Amino acids

FTIR spectroscopy can be used as an effective tool for exploring structural changes and functional mecha-nisms of bands that can be assigned to the vibrations of amino acids. Amino acids are very important components of tissues, playing the role of the building blocks of proteins. They are involved in metabolic processes (i.e., enzyme synthesis) at the molecular level. Therefore, conformational changes of amino acids may modificate the proper functioning of vital organs and cellular structure, i.e., the human nervous system, hormone production, and muscular structure.

2.2.1. ATR spectra of amino acids

ATR-FTIR spectra of amino acids, i.e., L-glycine (Gly), L-alanine (Ala) and L-phenylalanine (Phe) in aqueous solution contain many overlapped bands. In the case of strongly overlapped spectra first to fourth order derivatives can be used. In order to find detailed positions of vibrational bands, second order derivative of the basic absorption spectrum was calculated. Minima in this derivative spectrum indicate

Table 2. Major positions (in cm^{-1}) and tentative assignment of IR bands of aqueous L-glycine (Gly), L-alanine (Ala) and L-phenylalanine (Phe)

Gly	Ala	Phe	Assignments*
1614 *sh*	1620 *sh*	1628 *sh*	$\beta_{as}(NH_3^+)$
		1601 *sh*	8a, $\nu(C–C)_{ring}$
1601	1597	1583	$\nu_{as}(CO_2^-)$ + 8a, $\nu(C–C)_{ring}$
1509	1516	1528	$\beta_s(NH_3^+)$
		1496 *sh*	19a, $\nu(C–C)_{ring}$
		1448	19b, $\nu(C–C)_{ring} + \beta_s(CH_2)$
1412	1412	1408	$\nu_s(CO_2^-)$
	1373	1364	$\beta_s(CH_2)$
	1353		$\beta_s(CH_2)$
1331		1340	$\beta_s(CH_2)$
		1324	$\beta_s(CH_2)$
		1315 *sh*	14, $\nu(C–C)_{ring}$
		1209	13, $\nu(C–C)_{ring}$
		1197	9a, $\delta(C–H)_{ring}$
		1148	9b, $\delta(C–H)_{ring} + \rho(NH_3^+)$
1131	1138	1131 *sh*	$\rho(NH_3^+)$
		1115 *sh*, 1107	ν(ring–C)
		1078	18b, $\delta(C–H)_{ring}$
		1047	1, $\delta(C–C)_{ring}$
		1017	18a, $\delta(C–H)_{ring}$
		994	12, $\Delta(C–C)_{ring}$
		965	5, $\gamma(C–H)_{ring}$
		940	17a, $\gamma(C–H)_{ring}$
		918	17b, $\gamma(C–H)_{ring}$
929	919	913	$\gamma(CH_2)$

*Abbreviations: ν, stretching; β, in-plane bending; γ, out-of-plane bending; ρ, rocking; *s*, symmetrical; *as*, asymmetrical; *sh*, shoulder.

positions of band maxima of the basic absorption spectrum. Table 2 provides the assignments of vibrational modes of the L-gly, L-ala and L-phe aqueous solution arising in the 1800–700 cm^{-1} spectral region.

2.2.2. Studies of processes occurring in amino acids

2.2.2.1. Determination of pKa on the example of L-phenylalanine

Classical applications of molecular spectroscopy include determination of acid-base equilibrium constants pKa, using the ratio of the intensity bands corresponding to vibrations of specific functional groups [29]. The method is based on calculations of the ratio of band intensities typical of groups susceptible to amino acid ionization. A calculated intensity ratio corresponding to equal amounts of protonated and deprotonated forms is described by the pKa value – a negative algorithm of dissociation constants of carboxyl and amine groups in an amino acid molecule. For L-phenylalanine, four bands were chosen in order to determine the two pKa values, pK_1 and pK_2. These bands correspond to each ionized form of *L*-phenylalanine and their intensities modificate with changes of the pH value (table 3). The first band located at 1730 cm^{-1} was described as specific to the cationic form. Next, two peaks clearly arise near 1600 cm^{-1} and 1519 cm^{-1} as specific of the zwitterion. Finally, the band with absorption maximum at 1560 cm^{-1} was characterized as the typical anionic form [30]. As the next step, the intensities of the above-mentioned bands were measured and ratios of intensities of the proper bands were calculated. Two plots of the ratio of the intensity of the 1600 cm^{-1} to 1730 cm^{-1} component and the intensity of the 1560 cm^{-1} to 1519 cm^{-1} band versus the pH value were approximated. The band intensities of characteristic pure ionized forms were chosen based on the ATR-FTIR spectra of 0.25 mol/L *L*-phenylalanine at pH = 0.2, 8.0 and 13.0, respectively. From the mathematical point of view, the pK_1 corresponds to the value of pH, at which I_{1600}/I_{1730} ratio is equal to 6.25, which physically means equal concentrations of the zwitterionic and cationic forms. In the same way, the pK_2 value was found when the concentration of the anionic form was identical to the concentration of the zwitterionic form. From the fitting curves, the protonation equilibrium constants pK_1 and pK_2 were determined at 2.31 ± 0.13 and 9.28 ± 0.31, respectively, at 21 °C [33]. The fact that the obtained pKa values are comparable

to the literature data (near 2.16 and 9.18 [31], 2.16 and 9.24 [32], 2.20 and 9.31 [33]) is the evidence of the effectiveness of the method.

Table 3. Major positions (in cm^{-1}) and tentative assignment of IR bands of the typical cationic, zwitterionic, and anionic forms of L-phenylalanine selected to determine the pKa values [30]

Cationic form	Zwitterionic form	Anionic form	Assignments*
(pH = 0.2)	(pH = 7.9)	(pH = 13.0)	
1730			$\nu_{as}(C=O)$
	1600	1560	$\nu_{as}(CO_2^-)$
	1519		$\beta_s(NH_3^+)$

* Abbreviations: ν, stretching; β, in-plane bending; s, symmetrical; as, asymmetrical.

2.2.2.2. Aggregation of amino acids on the example of *L*-phenylalanine

The aggregation process refers to both amino acids and proteins. When seeking the most stable conformational state, molecules undergo a limited subset of potential transitions. The aggregation process is characterized by intermediate states. Stable, aggregated forms are formed due to intermolecular interactions that stabilize specific protein molecules. These interactions occur between partially folded protein conformations and account for about 50% interactions in the native structure of a protein.

The interactions that stabilize amino acid and protein conformations are mainly hydrogen bonding, polarization, electrostatic interactions, disulfide bridges, formation of complexes with metal ions and hydrophobic effects [34], [35]. Any structural change of water layers (i.e., dehydration) may lead to structural modifications of amino acid and protein molecules, resulting in vibration changes of their polar and nonpolar groups and, as a consequence, changes of intensity and position of IR spectral bands.

Dehydration of amino acid and protein surfaces (e.g., due to an external factor, including NIR radiation) weakens polar group interactions [36]. As a consequence, deprotonation of $-NH_3^+$ to $-NH_2$ and protonation of $-COO^-$ to $-COOH$ groups are observed in ATR-FTIR spectra. Therefore, secondary processes of amino acid conformational changes can occur [37]. After exposure to NIR, the concentration of cationic forms increases, which favours formation of strong hydrogen bonds between carboxyl $-COOH$ and carboxylate $-CO_2^-$ groups. Under these conditions, dimerization occurs, which is confirmed by quantum-

mechanical calculations [38]. Simultaneously, the concentration of anionic form increases, which leads to formation between $-NH_2$ and $-NH_3^+$ groups in the presence of water molecules. It should be noted, however, that in the presence of only zwitterionic ions, dimers would not be formed. Dimerization in amino acids can also occur under exposure to other kinds of radiation, i.e., UVA [39].

The fact that dehydration leads to aggregation is confirmed by the desiccation effect of *L*-phenylalanine solutions depending on the molecule charge of the amino acid associated with pH value of the solution. During water evaporation, amino acid surface becomes dehydrated through removal of the weakest-bound water. With reduction of the water/amino acid ratio, levels of neutral ions increase, resulting in dimer formation in the presence of water molecules [40].

The appearance of hydrogen bonds between the aminium and carboxylic groups may also lead to the formation of oligomers containing two identical amino acid molecules [41]. Similar dimers are analogically observed in aliphatic carboxylic acids at the 1700 cm^{-1} wavenumber in the IR spectrum [42], in derivatives of benzoic and toluic acids at 1715–1680 cm^{-1} [43], in benzoic and deuterobenzoic acids at 1699 cm^{-1} and 1697 cm^{-1} [44] or 3-furylpropenoic acid derivatives at 1684 cm^{-1} [45]. The presence of these H-bonded dimer forms can be enhanced by additional bands, such as: a broad medium intensity band in the 960–875 cm^{-1} region due to the OH–O deformation [42], [43] and the 1320–1220 cm^{-1} region, where multiple peaks of medium strength assigned to the C–O stretch appear in carboxylic acids [42]. This is confirmed by STEPHANIAN et al. [44], who observed during aggregation three additional bands for benzoic acid in the IR spectrum.

The band of amino acid dimer is observed in the 1680–1700 cm^{-1} region in the ATR spectrum [36], [40], [46]. The simultaneous presence of cationic and zwitterionic forms can lead to phenylalanine aggregation, which was demonstrated in the ATR spectrum as a new band at the 1673 cm^{-1} [36].

2.2.3. Amino acids in proteins

Amino acid side chains play important role in stabilizing protein structures. These properties and processes can be investigated by infrared spectroscopy at the molecular level. The presence of bands arising from amino acid side chains must be recognized before determining structural information from the shapes of Amide I and Amide II bands.

Vibrations of the side chain in the region between 1400 and 1800 cm^{-1} have been investigated (table 4) [47].

Table 4. Major positions (in cm^{-1}) and tentative assignment of IR bands of amino acids [47]

Amino acid	Theoretical region v [cm^{-1}]	Assignments*
Cys	2551	v(SH)
Asp	1716–1788	v(C=O)
	1402	v_s(COO$^-$)
	1375 or 1368, 1385	δ_s(CH$_3$)
	1264–1450	δ(COH)
	1120–1253	v(C–O)
Glu	1712–1788	v(C=O)
	1404	v_s(COO$^-$)
	1264–1450	δ(COH)
	1120–1253	v(C–O)
Asn	1677–1678	v(C=O)
Arg	1672–1673	v_{as}(CN$_3$H$_5^+$)
	1633–1636	v_s(CN$_3$H$_5^+$)
Gln	1668–1687	v(C=O)
	1586–1610	δ(NH$_2$)
	1410	v(C–N)
Lys	1626–1629	δ_{as}(NH$_3^+$)
	1526–1527	δ_s(NH$_3^+$)
Asn	1612–1622	δ(NH$_2$)
Asp	1574–1579	v_{as}(COO$^-$)
Glu	1556–1560	v_{as}(COO$^-$)
Trp	1622	v(C=C), v(C–C)
	1496	v(C–C), δ(C–H)
	1462	δ(C–H), v(C–C), v(C–N)
	1412–1435	δ(N–H), v(C–C), δ(C–H)
	1315–1350	δ(C–H)
	1276	δ(N–H), v(C–N), δ(C–H)
	1245	δ(C–H), v(C–C)
	1203	v(C–C)
	1092	δ(C–H), v(C–N)
	1064	δ(C–H), v(C–N), v(C–C)
	1012–1016	δ(C–H), v(C–C)
Phe	1494	v(C–C)$_{ring}$
	1445–1480	δ_{as}(CH$_3$)
His	1439	δ(CH$_3$), v(C–N)
	1217	δ(C–H), v(C–N), δ(N–H)
	1104	δ(C–H), v(C–N)
Pro	1400–1465	v(C–N)
	1425–1475	δ(CH$_2$)
Ser	1181–1420	δ(COH), v(C–O)
	1030	v(C–O)
	983	v(C–C)
Thr	1075–1150	v(C–O)

* Abbreviations: v, stretching; β, in-plane bending; s, symmetrical; as, asymmetrical.

2.3. Proteins

The structure of protein solution and interactions between water and protein molecules are investigated with the use of many physical methods, including increasing application of FTIR spectroscopy. FTIR spectroscopy provides information about the secondary structure content of proteins; unlike X-ray crystallography and NMR spectroscopy it concerns the tertiary structure. IR spectra of proteins can also learn about structure and environment of the protein backbone and of the amino acid side chains [47]. Therefore, protein secondary structure and reactions such as protein folding, unfolding and misfolding can be investigated from IR spectra [48]–[52]. Among IR techniques, attenuated total reflectance (ATR) FT-IR [53], [54] or single-pass ATR-FT-IR spectroscopy has also been demonstrated for the rapid determination of protein secondary structure [55]. ATR-FTIR spectroscopy has also been used to investigate the orientation and the accessibility to the water phase of the fusogenic domain of viral proteins [56]. Authors have suggested that the ATR method could also be used to detect changes located in the membrane domains and to identify intermediate structural states involved in the fusion process.

The peptide group, the structural repeat unit of proteins, gives up to 9 characteristic bands named amide A, B, and I–VII. The amide I band is the most intense and the most useful for conformational analysis of proteins. The amide I band is due primarily to the C=O stretching vibrations of the peptide linkages that constitute the backbone structure of proteins, combined with small contributions from in-plane N–H bending, out of phase C–N stretching and C–C–N bending vibrations. Broad bandwidth of the amide I arises from the presence of the various overlapping component bands that represents different secondary structures. It occurs in the region between 1600 and 1700 cm^{-1}. The amide II band is an out-of-phase combination of largely N–H in plane bending and C-N stretching and smaller contributions from C=O in-plane bending and N-C stretching. It is located between 1450 and 1600 cm^{-1}. The amide III band is the in-phase combination of N-H in-plane bending and C–N stretching. Less intensive is the contribution from C–C stretching and C–O bending. The amide III band can be found between 1250 and 1300 cm^{-1} [57]. Because the C=O and the N–H bonds are involved in the hydrogen bonding that takes place between the different components of secondary structure, the positions of the amides (I, II and III) bands can be sensitive to the secondary structure content of a protein.

2.3.1. Studies of processes occurring in proteins

2.3.1.1. Protein denaturation

Protein denaturation occurs when the equilibrium of protein/protein and protein/water interactions has been disturbed. Lesser extents of water/water molecule interactions in the bound water layer lead to increased water/protein interactions, which in turn may favour protein unfolding. Based on many studies, a protein denaturation model has been proposed. Thermal aggregation of proteins is usually characterized as an irreversible two-state model [58], [59].

Protein conformational structure and functions depend on the amount of bound water, which was investigated on the example of collagen [60]. In order to determine conformational changes, protein films on inorganic crystals were investigated depending on their hydration level, and a shift of the amide I band was observed. JAKOBSEN et al. studied the effects of pressure, pH value and nonaqueous solvents on an albumin film or salt solution to demonstrate that more ordered helical structures emerged when protein-surrounding water was bound [61]. Algorithms of free water subtraction from IR spectra of protein aqueous solutions were published by POWELL's and DOSUSSEAU's research teams [62], [63].

The original spectra have shown that the absorbance of the amide I band of proteins kept almost unchanged when the temperature was below 40–45 °C. At higher temperatures (below 60 °C) the amide I region was dominated by the α-helix band. Above 60 °C two new bands around 1620 cm^{-1} (strong) and 1680/90 cm^{-1} (weak) have been observed, i.e., in albumin [64], [65] and hemoglobin [65].

Processes of aggregation (especially uncontrolled aggregation) of proteins play an important role in metabolism of tissues and proper functioning of the whole organism. They have been associated with a series of diseases, including Alzheimer's, Parkinson's, Huntington's and anemia disease [65].

2.4. Tissues

IR absorption spectra provide information about the key biological components, such as proteins, lipids, nucleic acids and carbohydrates. Human cells, tissues and body fluids are generally composed of water, lipids, proteins, hydrocarbons and nucleic acids. Therefore, in IR absorption spectra of tissues, three major modes can be distinguished, i.e., lipid

(2800–3000 cm^{-1}), protein (1600–1700 cm^{-1}, 1500–1560 cm^{-1}) and nucleic acid (1000–1250 cm^{-1}) bands as well as additional bands typical of a specific tissue group.

2.4.1. Plasma

IR spectroscopy is a very good tool to study plasma and its content [66]. For example, FTIR spectra for the biomolecules appearing in plasma, such as: amino acids, fatty acids, albumin, glucose, fibrinogen, lactate, triglycerides, glycerol, urea, α_1-antitrypsin, α_2-macroglobulin, transferin, Apo-A1, Apo-B, Apo-C3, IgA, IgD, IgG1, IgG2, IgG3, IgG4, IgM, haptoglobin, α_1-acid glycoprotein, cholesterol, and cholesterol esters, were recorded. Serum components, such as glucose, total protein, cholesterol have also been obtained using mid-IR spectroscopy [67]. The mid-IR region has been shown to be useful in the identification of disease patterns (e.g., leukemia) using the FTIR spectrum of human plasma [68]. In the NIR region the concentrations of urea, glucose, protein and ketone in human urine can be measured [69].

In the FTIR spectrum of plasma solution we can expect bands associated mainly to Amide I and Amide II, that can be markers of conformational modifications in plasma [70]. Table 5 shows main components of those bands.

Table 5. Major positions (in cm^{-1}) and tentative assignment of IR Amide I and Amide II bands of plasma

	ν [cm^{-1}]	Theoretical region ν [cm^{-1}]	Assignments
Amide I	1694	1651–1694	β-sheet
	1681	1672–1694	disordered, β-turn
	1651	1642–1660	α-helix
	1635, 1629	1615–1638	β-sheet, (IgG$_3$) β-sheet, (IgG$_2$)
	1623	1630–1612	β-sheet – aggregation
Amide II	1542	1539–1554	disordered, β-sheet
	1534	1540–1523	β-sheet

2.4.2. Erythrocytes

Figure 2 shows the typical FTIR-ATR spectrum of erythrocytes with main absorption bands.

The two most intensive bands are centered at 1650 and 1545 cm^{-1} in the ATR-FTIR spectrum of erythrocyte aqueous solution. They correspond to the Amide I and Amide II. Both bands are representative of secondary structures of proteins. Amide I peak arises from C=O hydrogen bonded stretching vibrations, and

Amide II is attributed to CN stretching and CNH bending modes. Amide I and Amide II absorption bands are associated also with specific secondary substructures, such as α-helix, β-sheet, β-turn and random coil.
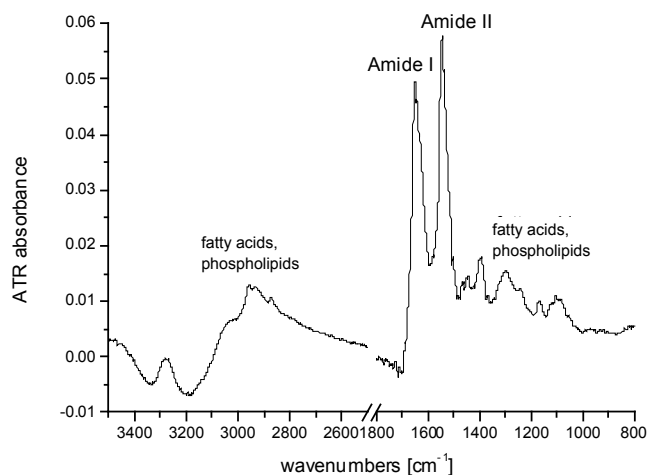

Fig. 2. FTIR-ATR spectrum of erythrocytes

The shoulder of the Amide I band, located between 1740 and 1725 cm^{-1} can originate from the carbonyl ester group in non-hydrogen bonded and hydrogen-bonded states, respectively.

Table 6. Major positions (in cm^{-1}) and tentative assignment of IR bands of erythrocytes

ν [cm^{-1}]	Assignments*	Secondary structures
3300	ν(NH), ν(OH)	water molecules, proteins, polysaccharides and carbohydrates
3017	ν(CH)	cholesterol esters, unsaturated fatty acids
2959	ν_{as}(CH$_3$)	phospholipids, cholesterol esters, fatty acids
2934	ν_{as}(CH$_2$)	phospholipids, long chain of fatty acids
1686	ν(C=O)	β-turn
1654		random coil
1648		α-helix
1644		random coil
1632		β-sheet
1613		β-strand
1545	β(N-H)	α-helix
1535		random coil
1518		β-sheet
1230	ν_{as}(PO^{2-})	phosphodiester groups of DNA
1085	ν_{s}(PO^{2-})	phosphodiester groups of DNA

* Abbreviations: ν, stretching; β, in-plane bending; s, symmetrical; as, asymmetrical.

Phosphate groups also characterise erythrocytes. The bands centered at 1230 cm^{-1} and 1085 cm^{-1} originate mainly from asymmetric and symmetric phosphate stretching modes, $v_{as}(PO_2^-)$ and $v_s(PO_2^-)$, respectively (table 6). They are attributed to the phosphodiester groups of nucleic acids from DNA. The composition of these bands also includes the COP stretching modes present in phosphorylated proteins and lipids.

In the range of higher wavenumbers we can expect the wide band at 3300 cm^{-1} that arises from the –NH and –OH vibrations of water molecules, proteins, polysaccharides and carbohydrates. Close to them stretching modes of the –CH$_2$ and –CH$_3$ groups, both symmetric and asymmetric, appear in the 2995–2800 cm^{-1} region [71].

When used for investigating erythrocytes and their oxidation process, infrared spectroscopy provides useful information about their conformational changes, membrane destruction and oxidative stress. For example, the method has helped explain the conformational order of phospholipids in cell membrane of erythrocytes as well as study the secondary structure of hemoglobin and the effects of various factors on its oxygen-binding capacity.

In the early 1990s, FIORINI [72] studied various lipid structures and membrane fluidities of five subgroups of human erythrocytes at different viability levels. While analyzing the 2922 cm^{-1} and 3011 cm^{-1} bands corresponding to asymmetric stretching modes of –CH$_2$ and =CH gropus, respectively, and comparing their optical densities, he found different lipid unsaturation and membrane fluidity levels among various groups of erythrocytes.

With the use of infrared spectroscopy, changes in phospholipid membrane domains and conformational changes resulting from oxidation processes in the course of sickle-cell anemia were also studied. Sickle-cell anemia belongs to the group of hereditary red blood cell diseases and results from abnormal hemoglobin structure caused by a gene mutation regarding the –CH$_2$ and =CH groups of the β-hemoglobin chain, which leads to an individual amino acid being replaced by another. These apparently slight changes in the hemoglobin structure are responsible for many abnormalities within erythrocyte membranes, including reduced deformability, water and ion transport changes, loss of lipid membranes and phospholipid asymmetry alterations. One of the reasons may be peroxidation of lipids induced by free radicals.

The ATR-FTIR technique is also a quick tool for analyzing hemoglobin of human blood [73] and measuring its concentration in whole blood [74]. Infrared difference spectroscopy was also used to correlate spectroscopic changes with biochemical and physical properties in diabetic platelets [75]. Several modifications in the IR spectra of the diabetic platelets associated with molecular vibrations of proteins, lipid or the glycosylation of platelets have been observed. Additionally, phase transitions in these isolated platelets membranes have been measured with both FTIR and differential scanning calorimetry (DSC) [76]. Platelets membranes give similar phase transitions. They are nearly indistinguishable from the intact cells. The study obtained by using FTIR spectroscopy fully confirms the results obtained by DSC. Changes of the band assigned to –CH$_2$ symmetric stretch in the hydrocarbon-stretching region in human platelets were observed. That band clearly shifted to higher wavenumbers, its intensity and bandwidth increased with increasing temperature. Spectral changes of the –CH$_2$ bands, which were observable by FTIR directly related to the membrane. Both fractions (the plasma membrane in internal membranes) gave very similar transitions.

2.5. Biomedical applications for diagnostic and prophylactic purposes

The knowledge provided by "conventional" medical diagnostic techniques might frequently be insufficient and require application of new investigation methods. Development of modern, particularly physical techniques opens up new ways for medical diagnostic methods. It allows us to obtain new information, i.e., about chemical composition of tissues and individual cells as well as molecular structures of biological systems, which has not been possible with the use of traditional diagnostic methods.

Vibrational spectroscopy techniques are worth consideration as they may be used for exploring disease processes. They offer many benefits compared to currently used diagnostic techniques, including significantly lower costs. As a specific analytical method, spectroscopy provides very quickly consistent information about biochemical compositions of tissues and cells. Its usefulness with regard to distinguishing between healthy and pathological tissues as well as disease classification and assessment of the disease progression has been frequently demonstrated. An additional combination of spectroscopy and microscopy techniques allows tissue microregions to be monitored and thereby, a biochemical analysis at a molecular level. In medical diagnostics, both near (NIR) and mid-infrared (MIR) spectroscopy techniques are applied. One of the more common techniques regarding

mid-infrared is ATR. This technique was used for detection of beta amyloid peptide (*Aβ*), whose aggregation in a human body leads to the Alzheimer disease [77]. Another example of ATR-FTIR spectroscopy application was a hemophilia diagnosis based on the test for blood clotting factor VIII binding capacity regarding the phosphatidylserine membrane [78]. NIR spectroscopy monitoring, in turn, allows us to detect life threatening situations due to harmful changes of oxygenated hemoglobin levels in tissues in the case of hypothermia or imperceptible pulse cases [79]. By means of the FTIR spectroscopy, changes in the course of the Parkinson [80] and Creutzfeldt–Jakob [81] diseases can be monitored.

2.5.1. Neoplastic lesions

Another important biological use of spectroscopic techniques is their potential application for distinguishing between neoplastic and non-neoplastic tissues as well as detection of precancerous cells.

In a study with the use of IR spectroscopy, a method for detecting differences in blood absorbance within IR ($1700–1600$ cm^{-1}) in blood smears of healthy people, women with fibroadenoma and patients with breast cancer was presented. In the presence of calcium cations, the IR spectra revealed significant differences, which might depend on conformational changes of a blood serum albumin molecule. The IR spectroscopic method used in investigations of human serum albumin molecules may be applied in breast cancer and fibroadenoma diagnostic tests [82].

Recently, Fourier-transform infrared (FTIR) spectroscopy has been employed to detect cancer tissues from non-cancerous ones in different types of cancer such as colon cancer, cervical cancer, gastric cancer and bowel disease [83]–[85]. Spectral parameters of malignant colonic tissue in comparison with normal colonic tissue have been measured. The conformational changes of the secondary structure of protein in Amide I band in normal and cancerous human colon tissue were observed: component of *α*-helixes increased, *β*-sheets and *β*-turns decreases and random coils were almost constant in cancer tissue [83].

Normal and cancerous breast tissue samples have been detected by FTIR spectroscopy with an attenuated total reflection (ATR) technique [86]. Results obtained have demonstrated that bands of protein, lipid, carbohydrate, and nucleic acid from cancerous samples are significantly different from the normal ones. ATR-FTIR spectroscopy has been utilized to estimate the secondary structure of amide I in normal and cancer tissue of human colon results, in which it

was shown that conformational changes of the secondary structure of protein in normal and cancerous human colon tissue are: increment in *β*-turns and composition of *α*-helixes and also decrement in *β*-sheets due to cancer while the composition of random coils would not be significantly different between normal and cancer tissues [83]. ATR method has also been useful for analysis of healthy and breast cancer affected people's hair. A significant increase of the ratio of *β*-sheet/disorder structures (relative to *α*-helix structures) and C–H lipid content of hair from breast cancerous patients has been observed. Thus, it was supposed that the presence of breast cancer appears to modify the hair growth process, resulting from changes in the composition and conformation of cell membrane and matrix materials of hair fiber [87]. FTIR spectroscopy has also been used to study glycogen levels in normal and cancerous tissues [88].

Acknowledgements

References

[1] Jackson M., Mantsch H.H., *FTIR spectroscopy in the clinical sciences*, [in:] *Biomedical Application of Spectroscopy. Advances in Spectroscopy*, Wiley&Sons, Chichester, UK, 1996, 25, 185–215.

[2] Tamm L.K., Tatulian S.A., *Infrared spectroscopy of proteins and peptides in lipid bilayers*, Quart. Rev. Biophys., 1997, 30, 365–429.

[3] Miles H.T., Frazier J., *Infrared spectroscopy of polynucleotides in the carbonyl region in water solution: A.U systems*, Biochemistry, 1978, 17, 2920–2927.

[4] Tsuboi M., *Infrared spectra and secondary structure of deoxyrybonucleic acid*, Progr. Theoret. Phys., 1961, 17, 99–107.

[5] Taillandier E., Liquier J., Ghomi M., *Conformational transitions of nucleic acids studied by IR and Raman spectroscopies*, J. Mol. Struct., 1989, 214, 185–211.

[6] Taillandier E., Liquier J., *Infrared spectroscopy of DNA*, Methods Enzymol., 1992, 211, 307–335.

[7] Pevsner A., Diem M., *Infrared Spectroscopic Studies of Major Cellular Components. Part II: The Effect of Hydration on the Spectra of Nucleic Acids*, Appl. Spectrosc., 2001, 55, 1502–1505.

[8] Banyay M., Sarkar M., Gräslund A., *A library of IR bands of nucleic acids in solution*, Biophys. Chem., 2003, 104, 477–488.

[9] Lee S.L., Debenedetti P.G., Errington J.R., *A Calorimetric and Spectroscopic study of DNA at low hydration*, J. Phys. Chem. B, 2004, 108, 3098–3106.

[10] Harmouchi M., Albiser G., Premilat S., *Changes of hydration during conformational transitions of DNA*, Eur. Biophys. J., 1990, 19, 87–89.

[11] MAKAROV V., PETTITT B.M., FEIG M., *Solvation and Hydration of Proteins and Nucleic Acids: A Theoretical View of Simulation and Experiment*, Acc. Chem. Res., 2002, 35, 376–384.

[12] KOSZTIN D., GUMPORT R., SCHULTEN K., *Probing the role of structural water in a duplex oligodeoxyribonucleotide containing a water-mimicking base analog*, Nucleic Acids Res., 1999, 27, 3550–3556.

[13] BLOOMFIELD V.A., CROTHERS D.M., TINOCO J., HEARST J.E., WEMMER, D.E., KOLLMAN P.A., TURNER D.H., *Nucleic Acids: Structures, Properties and Functions*, University Science Books, 2000, 476–487.

[14] KOPKA M.L., FRATINI A.V., DREW H.R., DICKERSON R.E., *Ordered Water Structure around a B-DNA dodecamer. A quantitative study*, J. Mol. Biol., 1983, 163, 129–146.

[15] SAENGER W., *Structure and Dynamics of Water Surrounding Biomolecules*, Ann. Rev. Biophys., 1987, 16, 93–114.

[16] VLIEGHE D., TURKENBURGB J.P., Van MEERVELTA L., *B-DNA at atomic resolution reveals extended hydration patterns*, Acta Crystallogr. D Biol. Crystallogr., 1999, 55, 1495–1502.

[17] FALK M., POOLE G.A., GOYMOUR C.G., *Infrared study of the state of water in the hydration shell of DNA*, Can. J. Chem., 1970, 48, 1536–1542.

[18] FEIG M., PETTITT M., *Modeling High-resolution Hydration Patterns in Correlation with DNA Sequence and Conformation*, J. Mol. Biol., 1999, 286, 1075–1095.

[19] BERMAN H.M., *Hydration of DNA*, Curr. Opin. Struc. Biol., 1991, 1, 423–427.

[20] WHELAN D.R., BAMBERY K.R., HERAUDM P., TOBIN M.J., DIEM M., McNAUGHTON D, WOOD B.R., *Monitoring the reversible B to A-like transition of DNA in eukaryotic cells using Fourier transform infrared spectroscopy*, Nucleic Acids Res., 2011, 39, 13, 5439–5448.

[21] FALK M., HARTMAN K., LORD K., *Hydration of Deoxyribonucleic Acid. II. An Infrared Study*, J. Am. Chem. Soc., 1963, 85, 4, 387–391.

[22] DUGUID J., BLOOMFIELD V.A., BENEVIDES J., THOMAS Jr. G.J., *Raman spectroscopy of DNA-metal complexes. I. Interactions and conformational effects of the divalent cations: Mg, Ca, Sr, Ba, Mn, Co, Ni, Cu, Pd, and Cd*, Biophys. J., 1993, 65, 5, 1916–1928.

[23] HACKL E.V., KORNILOVA S.V., KAPINOS L.E., ANDRUSHCHENKO V.V., GALKIN V.L., GRIGORIEV D.N., BLAGOI Yu.P., *Study of Ca^{2+}, Mn^{2+} and Cu^{2+} binding to DNA in solution by means of IR spectroscopy*, J. Mol. Struct., 1997, 408–409, 229–232.

[24] AHMAD R., ARAKAWA H., TAJMIR-RIAHI H.A., *A Comparative Study of DNA Complexation with Mg(II) and Ca(II) in Aqueous Solution: Major and Minor Grooves Bindings*, Biophys. J., 2003, 84, 2460–2466.

[25] TAILLANDIER E., LIQUIER J., TABOURY J.A., *Infrared spectral studies of DNA conformations*, [in:] *Advances in Infrared and Raman Spectroscopy*, R.J.H. Clark, R.E. Hester (eds.), Wiley-Heyden, New York, 1985, 65–114.

[26] ALEX S., DUPUIS P., *FTIR and Raman investigation of cadmium binding by DNA*, Inorg. Chim. Acta, 1989, 157, 271–281.

[27] TAJMIR-RIAHI H.A., NAOUI M., AHMAD R., *The effects of Cu^{2+} and Pb^{2+} on the solution structure of calf thymus DNA: DNA condensation and denaturation studied by Fourier transform IR difference spectroscopy*, Biopolymers, 1993, 33, 1819–1827.

[28] OUAMEUR A.A., ARAKAWA H., AHMAD R., NAOUI M., TAJMIR-RIAHI H.A., *A Comparative study of Fe(II) and Fe(III) interactions with DNA duplex: major and minor grooves bindings*, DNA Cell. Biol., 2005, 24, 394–401.

[29] MERLIN J.C., THOMAS E.W., PETIT G. J., *Resonance Raman study of phenylhydrazonopropanedinitriles*, Can. J. Chem., 1985, 63, 1840–1844.

[30] OLSZTYŃSKA S., KOMOROWSKA M., VRIELYNCK L., DUPUY N., *Vibrational spectroscopic study of L-phenylalanine: Effect of pH*, Appl. Spectrosc., 2001, 55, 901–907.

[31] WALLACH J., *Les enzymes*, Nathan Ed., Paryż, 1997.

[32] BARBOIU M., GUIZARD C., LUCA C., ALBU B., HOVNANIAN N., PALMERI J., *A new alternative to amino acids transport: facilitated transport of L-phenylalanine by hybrid siloxane membranes containing a fixed site macrocyclic complexant*, J. Membrane Sci., 1999, 161, 193–206.

[33] DAWSON R.M.C., ELLIOTT D.C., ELLIOTT W.H., JONES K.M., *Data for Biochemical Research*, 3 ed., Oxford Science Publications, 1986.

[34] RAJKUMAR B.J.M., RAMAKRISHNAN V., RAJARAM R.K., *Infrared and Raman spectra of DL-aspartic acid nitrate monohydrate*, Spectrochim. Acta Part A, 1998, 54, 1527–1532.

[35] MUTA H., KOJIMA R., KAWAUCHI S., TACHIBANA A., SATOH M., *Ion-specificity for hydrogen-bonding hydration of polymer: an approach by ab initio molecular orbital calculations*, J. Mol. Struct. Theochem., 2001, 539, 219–236.

[36] OLSZTYŃSKA-JANUS S., SZYMBORSKA K., KOMOROWSKA M., LIPIŃSKI J., *Usefulness of spectroscopy for biomedical engineering*, Acta Bioeng. Biomech., 2008, 10, 3, 45–49.

[37] OLSZTYŃSKA S., DOMAGALSKA B.W., KOMOROWSKA M., *Aggregation of L-phenylalanine amino acid*, [in:] *Surfactants and dispersed systems in theory and practice*, K.A. Wilk (ed.), Oficyna Wydawnicza Politechniki Wrocławskiej, Wrocław, Poland, 2003, 405–409.

[38] OLSZTYŃSKA-JANUS S., SZYMBORSKA K., KOMOROWSKA M., LIPIŃSKI J., *Conformational changes of L-phenylalanine – near infrared-induced mechanism of dimerization: B3LYP studies*, J. Mol. Struct. Theochem., 2009, 911, 1–3, 1–7.

[39] TANAKA M., KANEKO F., KOKETSU T., NAKAGAWA K., YAMADA T., *Fragmentation and dimerization of aliphatic amino acid films induced by vacuum ultraviolet irradiation*, Radiat. Phys. Chem., 2008, 77, 1164–1168.

[40] OLSZTYŃSKA-JANUS S., DUPUY N., VRIELYNCK L., KOMOROWSKA M., *Water evaporation analysis of L-phenylalanine from initial aqueous solutions to powder state by vibrational spectroscopy*, Appl. Spectrosc., 2006, 60, 9, 1040–1053.

[41] KUZNETSOVA S.E., BURYAK K.A., *Experimental and theoretical investigation of amino acids dimers and associates adsorption on carbon surface*, Colloids Surf. A Physicochem. Eng. Aspects, 2011, 383, 73–79.

[42] SOKRATES G., *Infrared Characteristic Group Frequencies. Tables and Charts*, John Wiley and Sons, New York, 1994.

[43] COLTHUP N.B., DALY L.H., WIBERLEY S.E., *Introduction to Infrared and Raman Spectroscopy*, 3rd ed., Academic Press, New York, 1990.

[44] STEPANIAN S.G., REVA I.D., RADCZENKO E.D., SHEINA G.G., *Infrared spectra of benzoic acid monomers and dimers in argon matrix*, Vib. Spectrosc., 1996, 11, 123–133.

[45] KISS J.T., FELFOLDI K., PAKSI Z., PALINKO I., *Structure-forming properties of 3-furylpropenoic acid derivatives in solution and in the solid state*, J. Mol. Struct., 2003, 651–653, 253–258.

[46] PARKER F.S., *Application of infrared Raman and resonance Raman spectroscopy in biochemistry*, Plenum Press, New York, 1983.

[47] BARTH A., *The infrared absorption of amino acid side chains*, Prog. Biophys. Mol. Biol., 2000, 74, 141–173.

[48] HARRIS P.I., CHAPMAN D., *Does Fourier-transform infrared spectroscopy provide useful information on protein structures?*, Trends. Biochem. Sci., 1992, 17, 328–333.

[49] JACKSON M., MANTSCH H.H., *The use and misuse of FTIR spectroscopy in the determination of protein structure*, Crit. Rev. Biochem. Mol. Biol., 1995, 30, 95–120.

[50] GOLDBERG M.E., CHAFFOTTE A.F., *Undistorted structural analysis of soluble proteins by attenuated total reflectance infrared spectroscopy*, Protein Sci., 2005, 14, 2781–2792.

[51] GRDADOLNIK J., *Saturation effects in FTIR spectroscopy: intensity of Amide I and Amide II bands in protein spectra*, Acta Chim. Slov., 2003, 50, 777–788.

[52] GRDADOLNIK J., MARÉCHAL Y., *Bovine serum albumin observed by infrared spectrometry*. I. *Methodology, structural investigation, and water uptake*, Biopolymers (Biospectroscopy), 2001, 62, 40–53.

[53] PEVSNER A., DIEM M., *Infrared spectroscopic studies of major cellular components*. Part I: *The effects of hydration on the spectra of proteins*, Appl. Spectrosc., 2001, 55, 788–793.

[54] WANG S.-L., WEI Y.-S., LIN S.-Y., *Subtractive similarity method used to study the infrared spectra of proteins in aqueous solution*, Vib. Spectr., 2003, 31, 313–319.

[55] SMITH B.M., OSWALD L., FRANZEN S., *Single-pass attenuated total reflection Fourier transform infrared spectroscopy for the prediction of protein secondary structure*, Anal. Chem., 2002, 74, 3386–3391.

[56] MARTIN I., GOORMAGHTIGH E., RUYSSCHAERT J.-M., *Attenuated total reflection IR spectroscopy as a tool to investigate the orientation and tertiary structure changes in fusion proteins*, Biochim. Biophys. Acta, 2003, 1614, 97–103.

[57] FABIAN H., MÄNTELE W., *Infrared spectroscopy of proteins*, [in:] *Handbook of Vibrational Spectroscopy*, Chalmers J.M., Griffiths P.R. (eds.), John Wiley&Sons, Chichester, UK, 2002, 3399–3425.

[58] FING A.L., *Protein aggregation: folding aggregates inclusion bodies and amyloid*, Fold. Des., 1998, 3, R9–R23.

[59] DONG A., RANDOLPH T.W., CARPENTER J.F., *Entrapping intermediates of thermal aggregation in a-helical proteins with low concentration of guanidine hydrochloride*, J. Biol. Chem., 2000, 275, 27689–27693.

[60] LAZAREV Y.A., GRISHKOVSKY B.A., KHROMOVA T.B., LAZAREVA A.V., GRECHISHKO V.S., *Bound water in the collagen-like triple-helical structure*, Biopolymers, 1992, 32, 189–195.

[61] JAKOBSEN R.J., WASACZ F.M., BRASCH J.W., SMITH K.B., *The relationship of bound water to the IR amide I bandwidth of albumin*, Biopolymers, 1986, 25, 639–654.

[62] POWELL J.R., WASACZ F.M., JAKOBSEN R.J., *An algorithm for the reproducible spectral subtraction of water from the FTIR spectra of proteins in dilute solutions and adsorbed monolayers*, Appl. Spectrosc., 1986, 40, 339–344.

[63] DOUSSEAU F., THERRIEN M., PÉZOLET M., *On the spectral subtraction of water from the FT-IR spectra of aqueous solutions of proteins*, Appl. Spectrosc., 1989, 43, 538–542.

[64] DONG A., MEYER J.D., BROWN J.L., MANNING M.C., CARPENTER J.F., *Comparative FTIR and CD spectroscopic analysis of alpha a1-proteinase inhibitor and ovalbumin in aqueous solution*, Arch. Biochem. Biophys., 2000, 383, 148–155.

[65] YAN Y.-B., WANG Q., HE H.-W., ZHOU H.-M., *Protein Thermal Aggregation Involves Distinct Regions: Sequential Events in the Heat-Induced Unfolding and Aggregation of Hemoglobin*, Biophys. J., 2004, 86, 1682–1690.

[66] PETIBOIS C., DELERIS G., *Applications of FT-IR spectrometry to plasma contents analysis and monitoring*, Vib. Spectrosc., 2003, 32, 129–136.

[67] PETIBOIS C., CAZORLA G., GIN H., DELERIS G., *Differentiation of populations with different physiologic profiles by plasma Fourier-transform infrared spectra classification*, J. Lab. Clin. Med., 2001, 137, 184–190.

[68] ERUKHIMOVITCH V., TALYSHINSKY M., SOUPRUN Y., HULEIHEL M., *FTIR spectroscopy examination of leukemia patients plasma*, Vib. Spectrosc., 2006, 40, 40–46.

[69] STAIB A., DOLENKO B., FINK D.J., FRUH J., NIKULIN A.E., OTTO M., PESSIN-MINSLEY M.S., QUARDER O., SOMORJAI R., THIENEL U., WERNER G., *Disease pattern recognition testing for rheumatoid arthritis using infrared spectra of human serum*, Clin. Chim. Acta, 2001, 308, 79–89.

[70] BARTH A., *Infrared Spectroscopy of Proteins*, Biochim. Biophys. Acta, 2007, 1767, 1073–1101.

[71] PETIBOIS C., DELERIS G., *Oxidative stress effects on erythrocytes determined by FT-IR spectrometry*, Analyst, 2004, 129, 912–916.

[72] FIORINI R., CURATOLA G., KANTAR A., GORGI P.L., BERTOLI E., FANFANI F., *Steady state fluorescence polariazation and Fourier transform infrared spectroscopy studies on membranes of functionally senescent human erythrocytes*, Biochem. Int., 1990, 20, 715–724.

[73] TAO P., AIHONG P., WENJIE H., *Model Optimization and Stability of Hemoglobin Analysis in Human Soluble Blood Samples by FTIR/ATR Spectroscopy*, Appl. Mech. Materials, 2011, 55–57, 1168–1171.

[74] YIN H., PAN T., TIAN P.L., *The rapid quantitative analysis for the human blood hemoglobin applied through the FTIR/ATR spectrum*, Chin. J. Spectrosc. Lab., 2009, 26, 2, 431–436.

[75] LIU K.-Z., BOSE R., MANTSCH H.H., *Infrared spectroscopic study of diabetic platelets*, Vib. Spectrosc., 2002, 28, 131–136.

[76] CROWE J.H., TABLIN F., TSVETKOVA N., OLIVER A.E., WALKER N., CROWE L.M., *Are Lipid Phase Transitions Responsible for Chilling Damage in Human Platelets?*, Cryobiology, 1999, 38, 180–191.

[77] KLEIREN E., RUYSSCHAERT M.J., GOORMAGHTIGH E., RAUSSENS V., *Development of a quantitative and conformation-sensitive ATR-FTIR biosensor for Alzheimer's disease: The effect of deuteration on the detection of the Aβ peptide*, Spectroscopy, 2010, 24, 61–66.

[78] AAMOUCHE A., GOORMAGHIGH E., *FTIR-ATR biosensor based on self-assembled phospholipids surface: Haemophilia factor VIII diagnosis*, Spectroscopy, 2008, 22, 223–234.

[79] TRAFIDŁO T., GASZYŃSKI T., *NIRS – spektroskopia bliskiej podczerwieni jako wielofunkcyjna metoda monitorowania miejscowej oksygenacji tkankowej w anestezjologii i ratownictwie*, Anestezjologia i Ratownictwo, 2009, 351–359.

[80] RAMAKRISHNAN M., JENSEN P.H., MARSH D., *Association of α-Synuclein and Mutants with Lipid Membranes: Spin-Label ESR and Polarized IR*, Biochemistry, 2006, 45, 3386–3395.

[81] THOMZIG A., SPASSOV S., FRIEDRIECH M., NAUMANN D., BEEKES M., *Discriminating scrapie and bovine spogiform encephalopathy isolates by infrared spectroscopy of pathological prion protein*, J. Biol. Chem., 2004, 279, 33847–33854.

[82] Pershko N., Burlaka D., Korizkaya L., Levtchenko O., Pelevin S., Sidorenko M., *The IR-spectroscopy of blood as a possible diagnostic approach for breast cancer and fibro-adenomatous diagnostics*, Annales Universitatis Marie Curie-Skłodowska Lublin – Polonia, XXI, 2008, 2, 42.

[83] Chen Y.J., Hsieh Y.W., Cheng Y.D., Liao C.C., *Study on the secondary structure of protein in amide I band from human colon cancer tissue by Fourier-transform infrared spectroscopy*, Chang Gung Med. J., 2001, 24, 541–546.

[84] Fujioka N., Morimoto Y., Arai T., Kikuchi M., *Discrimination between normal and malignant human gastric tissues by Fourier transform infrared spectroscopy*, Cancer Det. Prev., 2004, 28, 32–36.

[85] Argov S., Sahu R.K., Bernshtain E., Salman A., Shohat G., Zelig U., Mordechai S., *Inflamatory bowel diseases as an intermediate stage between normal and can-cer: A FTIR microspectroscopy approach*, Biopolymers, 2004, 75, 5, 384–392.

[86] Khanmohammadi M., Ansari M.A., Bagheri Garmarudi A., Hassanzadeh G., Garoosi G., *Cancer Diagnosis by Discrimination between Normal and Malignant Human Blood Samples Using Attenuated Total Reflectance-Fourier Transform Infrared Spectroscopy*, Cancer Invest, 2007, 25, 397–404.

[87] Lyman D.J., Murray-Wijelath J., *Fourier Transform Infrared Attenuated Total Reflection Analysis of Human Hair: Comparison of Hair from Breast Cancer Patients with Hair from Healthy Subjects*, Appl. Spectrosc., 2005, 59, 1, 26–32.

[88] Yano K., Sakamoto Y., Hirosawa N., Tonooka S., Katayama H., Kumaido K., Satomi A., *Applications of Fourier transform infrared spectroscopy, Fourier transform infrared microscopy and near infrared spectroscopy to cancer research*, Spectroscopy, 2003, 17, 2–3, 315–321.